

Active Metamaterial Based Terahertz Polarimeter for Spectroscopic Detection of Chemical and Biological Hazards

**by Grace D. Metcalfe, Michael Wraback,
Richard D. Averitt, and Xin Zhang**

ARL-TR-6913

April 2014

NOTICES

Disclaimers

The findings in this report are not to be construed as an official Department of the Army position unless so designated by other authorized documents.

Citation of manufacturer's or trade names does not constitute an official endorsement or approval of the use thereof.

Destroy this report when it is no longer needed. Do not return it to the originator.

Army Research Laboratory

Adelphi, MD 20783-1197

ARL-TR-6913

April 2014

Active Metamaterial Based Terahertz Polarimeter for Spectroscopic Detection of Chemical and Biological Hazards

Grace D. Metcalfe and Michael Wraback
Sensors and Electron Devices Directorate, ARL

Richard D. Averitt and Xin Zhang
Boston University
Department of Physics
590 Commonwealth Avenue
Boston, MA 02215 USA

REPORT DOCUMENTATION PAGE			Form Approved OMB No. 0704-0188		
<p>Public reporting burden for this collection of information is estimated to average 1 hour per response, including the time for reviewing instructions, searching existing data sources, gathering and maintaining the data needed, and completing and reviewing the collection information. Send comments regarding this burden estimate or any other aspect of this collection of information, including suggestions for reducing the burden, to Department of Defense, Washington Headquarters Services, Directorate for Information Operations and Reports (0704-0188), 1215 Jefferson Davis Highway, Suite 1204, Arlington, VA 22202-4302. Respondents should be aware that notwithstanding any other provision of law, no person shall be subject to any penalty for failing to comply with a collection of information if it does not display a currently valid OMB control number.</p> <p>PLEASE DO NOT RETURN YOUR FORM TO THE ABOVE ADDRESS.</p>					
1. REPORT DATE (DD-MM-YYYY) April 2014		2. REPORT TYPE Final		3. DATES COVERED (From - To) March 2010 to September 2013	
4. TITLE AND SUBTITLE Active Metamaterial Based Terahertz Polarimeter for Spectroscopic Detection of Chemical and Biological Hazards			5a. CONTRACT NUMBER		
			5b. GRANT NUMBER		
			5c. PROGRAM ELEMENT NUMBER		
6. AUTHOR(S) Grace D. Metcalfe, Michael Wraback, Richard D. Averitt, and Xin Zhang			5d. PROJECT NUMBER		
			5e. TASK NUMBER		
			5f. WORK UNIT NUMBER		
7. PERFORMING ORGANIZATION NAME(S) AND ADDRESS(ES) U.S. Army Research Laboratory ATTN: RDRL-SEE-M 2800 Powder Mill Road Adelphi, MD 20783-1197			8. PERFORMING ORGANIZATION REPORT NUMBER ARL-TR-6913		
9. SPONSORING/MONITORING AGENCY NAME(S) AND ADDRESS(ES) Defense Threat Reduction Agency 8725 John J. Kingman Road Stop 6201/3265D Fort Belvoir, VA 22060-6201			10. SPONSOR/MONITOR'S ACRONYM(S)		
			11. SPONSOR/MONITOR'S REPORT NUMBER(S)		
12. DISTRIBUTION/AVAILABILITY STATEMENT Approved for public release; distribution unlimited.					
13. SUPPLEMENTARY NOTES Author's email: grace.d.metcalfe.civ@mail.mil					
14. ABSTRACT Polarimetry is the analysis of the polarization state of radiation following interaction with a sample. It has distinct advantages in comparison to techniques that solely measure changes in amplitude. There has been virtually no polarimetry work at terahertz (THz) frequencies because, until recently, it has been difficult to create components to control the polarization and the amplitude of THz radiation at modulation rates sufficient for potential high-sensitive applications. Our project attempted to develop the essential components such that THz polarimetry may enhance the ability to study previously unexploited spectral responses in the THz frequency range of molecules to allow for identification of chemical or biological threat analytes.					
15. SUBJECT TERMS metamaterials, terahertz, polarimeter					
16. SECURITY CLASSIFICATION OF:			17. LIMITATION OF ABSTRACT UU	18. NUMBER OF PAGES 24	19a. NAME OF RESPONSIBLE PERSON Grace D. Metcalfe
a. REPORT Unclassified	b. ABSTRACT Unclassified	c. THIS PAGE Unclassified			19b. TELEPHONE NUMBER (Include area code) (301) 394-2864

Contents

List of Figures	iv
1. Introduction	1
2. Major Goal	1
3. Accomplishments/New Findings	1
4. Opportunities for Training and Professional Development Provided by the Project	10
5. Dissemination to Communities of Interest	11
6. Personnel Supported	11
7. Impact	11
7.1 Publications	11
7.2 Participation/Presentations at Meetings, Conferences, Seminars, etc.....	13
7.3 New Discoveries, Inventions, or Patent Disclosures.....	14
7.4 Honors/Awards.....	14
7.5 Courses Taught.....	14
8. Conclusion	15
List of Symbols, Abbreviations, and Acronyms	16
Distribution List	17

List of Figures

Figure 1. (Left) Unit cell ($195\ \mu\text{m} \times 234\ \mu\text{m}$) for reflecting HWP at 0.350 THz with 45° angle of incidence. (Right) Simulation results of throughput magnitudes, phase difference, residual polarization percentage, and converted polarization percentage.	2
Figure 2. (a) Image of the reflection-mode THz polarimeter incorporating wide bandwidth photomixers with high resolution Schottky diodes. (b) Plot of the SNR performance of the photomixers and Band 1 and 2 Schottky diodes.	2
Figure 3. (Left) Schematic of experimental setup for metamaterial characterization. (Right) Experimental results compared with Jones matrix modeling of the HWP at 0.350 THz.	3
Figure 4. Experimental results compared with Jones matrix modeling of the QWP at 0.350 THz.	3
Figure 5. Illustrations of an (a) optically and (b) electrically modulated QWPs.	4
Figure 6. Stokes parameters of the optically modulated QWP shown in figure 5a.	5
Figure 7. Stokes parameters of the electrically modulated QWP shown in figure 5b.	5
Figure 8. (a) Illustration of the 3-D electrically modulated QWP and (b) simulated transverse magnetic (TM) and transverse electric (TE) mode throughput and phase shift.	6
Figure 9. (a) Image of the fabricated optically controlled PA. (b) Simulated and (c) measured reflectivity from the first generation optically controlled PA. A 532-nm CW laser was used for optical biasing.	7
Figure 10. (a) Image of the fabricated electrically controlled PA and (b) schematic of the unit cell, and plot of the simulated absorption.	8
Figure 11. Plot of the experimentally measured reflectivity from the second-generation optically controlled perfect absorber.	8
Figure 12. (a) Illustration and scanning electron microscopy (SEM) image of third-generation optically controlled PA. (b) Experimental and (c) simulated performance of the PA.	9
Figure 13. Image of the optically controlled (a) unit cell and (b) array of the dual gap frequency tunable metamaterial. Plot of the (a) measured and simulated transmission spectra.	10

1. Introduction

Polarimetry is the analysis of the polarization state of radiation following interaction with a sample. It has distinct advantages in comparison to techniques which solely measure changes in amplitude. There has been virtually no polarimetry work at terahertz (THz) frequencies because, until recently, it has been difficult to create components to control the polarization and the amplitude of THz radiation at modulation rates sufficient for potential high-sensitive applications. Our project attempted to develop the essential components such that THz Polarimetry may enhance the ability to study previously unexploited spectral responses in the THz frequency range of molecules to allow for identification of chemical or biological threat analytes.

2. Major Goal

The major goal of our effort was to create functionally active metamaterial devices to enable real-time control of the polarization of THz radiation for enhanced chemical and biological threat detection based on polarimetric signatures.

3. Accomplishments/New Findings

Two approaches to actively manipulating THz polarization were investigated using (1) waveplates and (2) perfect absorbers. In regard to the waveplates, we successfully designed, modeled, fabricated, and characterized low profile, high efficiency quarter waveplates (QWPs) and half waveplates (HWPs) operating in the THz frequency range. One significant finding during our program includes a considerable increase in throughput by using reflection, instead of transmission, mode THz waveplates. For example, figure 1 shows a static configuration HWP, which will rotate linear polarized light or convert the handedness of circularly polarized light. It consists of a periodic gold/polyimide composite with a physical thickness of $\lambda/10$ and is designed to operate in reflection mode. It has an intensity throughput of 80% at the design frequency of 0.350 THz, which is quite high in comparison to transmissive THz components, which typically suffer a large insertion loss due to Fresnel reflections. The waveplate maintains the high degree of polarization conversion and ease of fabrication of our previous transmissive waveplates, but also has a greatly increased efficiency. Specifically, the reflection mode waveplate exhibits an increased intensity throughput efficiency (80% in comparison to 50%). These structures are

compact, flexible, and easily fabricated over large areas using standard microfabrication processing. The waveplate was simulated using CST Microwave Studio (figure 1) and designed for operation at 0.350 THz with a 45° angle of incidence. The operation frequency was chosen to be in an atmospheric window (between water absorption lines), but can be designed to function at any frequency. Simulations indicate a half wave rotation of over 99% of the reflected THz radiation from 0.320–0.372 THz.

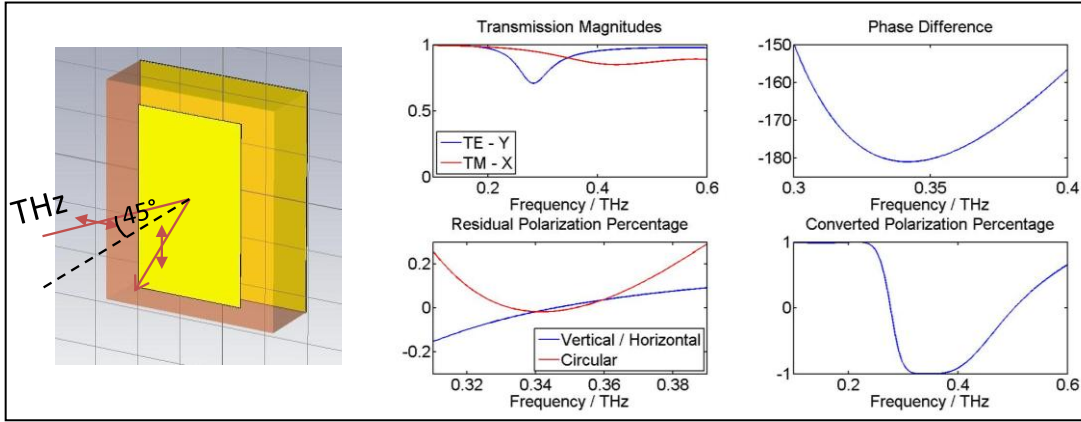


Figure 1. (Left) Unit cell (195 μm x 234 μm) for reflecting HWP at 0.350 THz with 45° angle of incidence. (Right) Simulation results of throughput magnitudes, phase difference, residual polarization percentage, and converted polarization percentage.

To validate the simulated results, the sample was fabricated and characterized using our continuous-wave (CW) high-resolution reflection-mode THz spectroscopy system pictured in figure 2a. The system consists of a pair of photomixers with a <2 MHz resolution and wide continuous tuning range of 0.09 to 1.2 THz. To enhance the dynamic range, Schottky diodes with a higher resolution (1 kHz) and higher signal-to-noise ratio (SNR) were incorporated into the photomixer system. As shown in figure 2b, the Schottky diodes cover the 0.33 to 0.50 THz (Band 1) and 0.50 to 0.73 THz (Band 2) regions. All THz transmitters and receivers were leveraged from other U.S. Army Research Laboratory (ARL) THz programs.

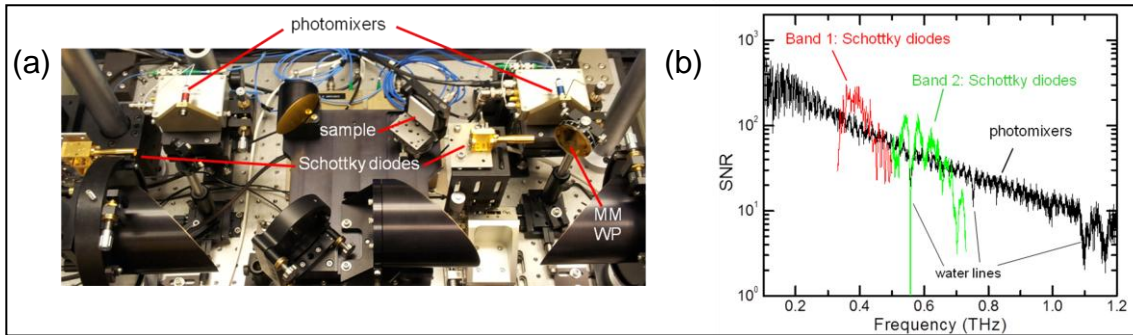


Figure 2. (a) Image of the reflection-mode THz polarimeter incorporating wide bandwidth photomixers with high resolution Schottky diodes. (b) Plot of the SNR performance of the photomixers and Band 1 and 2 Schottky diodes.

The waveplate was placed on a sample holder with an incident s-polarized beam at a 45° angle and illuminated by a 0.350 THz CW beam (figure 3). The analyzer was then rotated while the detected p-polarized signal amplitude was recorded as a function of angle. Figure 3 shows the results (points) plotted against modeling (solid line) and clearly demonstrates both the conversion, and extinction, of the incident polarization as a function of analyzer rotation. The modeling is based on Jones matrix analysis, which we developed specifically for our experiments, and indicates a π phase shift, as expected, for the HWP. Similar data and modeling for the QWP, which will convert linearly (circularly) polarized to circularly (linearly) polarized light, are shown in figure 4. Data analysis shows a $\pi/1.6$ phase shift.

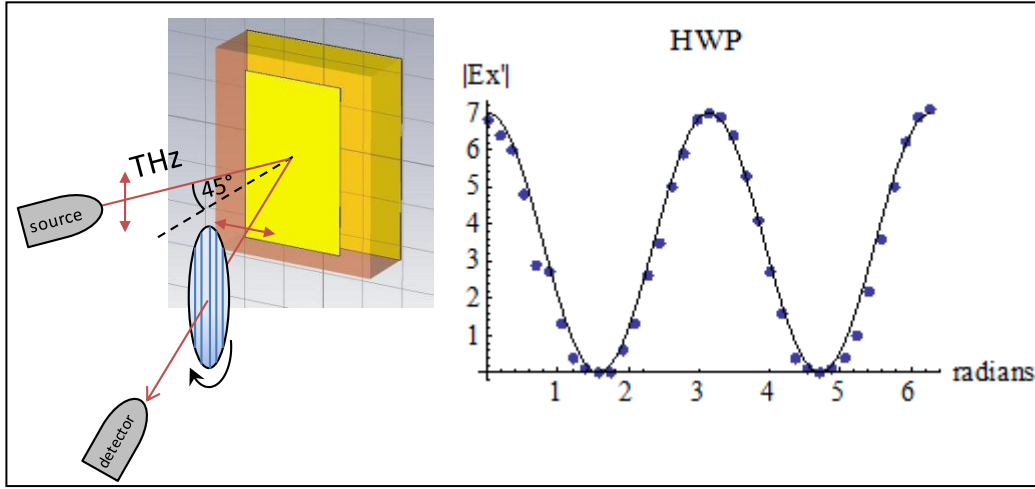


Figure 3. (Left) Schematic of experimental setup for metamaterial characterization. (Right) Experimental results compared with Jones matrix modeling of the HWP at 0.350 THz.

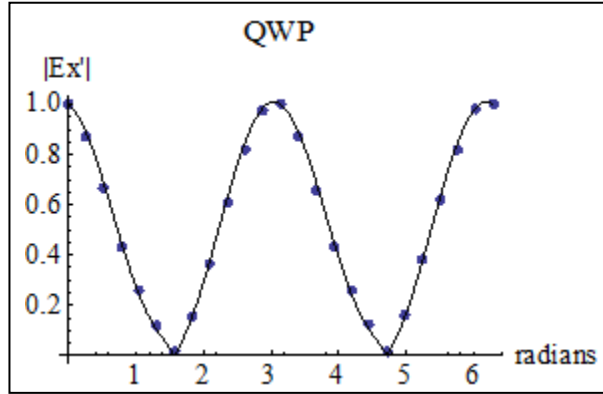


Figure 4. Experimental results compared with Jones matrix modeling of the QWP at 0.350 THz.

While these structures were designed for 0.350 THz, it is worth noting that this frequency is easily adjustable by appropriately scaling the waveplate dimensions. Due to the ease of their scaling, robust nature, and incredible simplicity, reflecting waveplates are an attractive choice for use in CW THz systems.

For active polarization control using metamaterial-based waveplates, there are two main issues. Firstly, a significant phase shift must be obtained. This was accomplished in the static configuration described above. Secondly, we must be able to sufficiently modulate the phase shift to achieve appropriate polarization control. One can accomplish this by applying an optical or electrical bias to turn “on” and “off” the device. Figure 5 shows the unit cell of an (a) optically and (b) electrically modulated QWP consisting of an electrical split-ring resonator (SRR). In the optical case, an external optical beam creates carriers to shunt the capacitive gap and thereby turns “off” the SRR resonance. In the electrical case, a reverse bias applied to a Schottky-Ohmic contact depletes in-gap carriers to reduce the substrate conductivity at the split gap and turn “on” the SRR resonance.

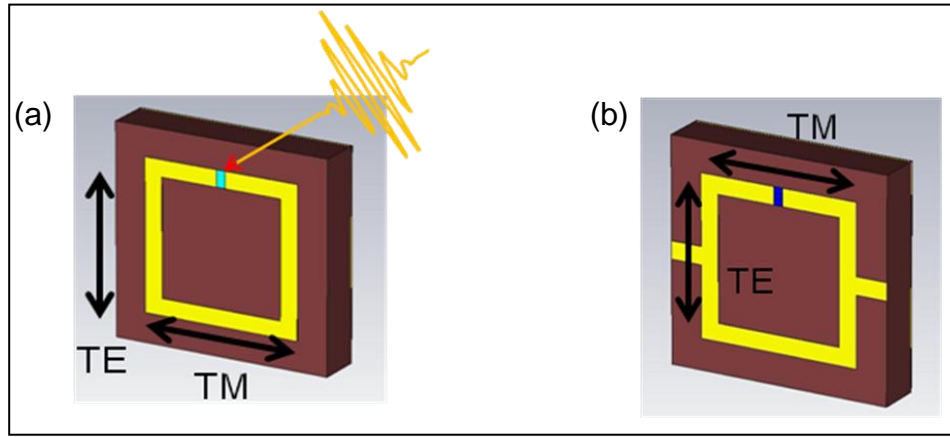


Figure 5. Illustrations of an (a) optically and (b) electrically modulated QWPs.

Simulations of the optically controlled QWPs demonstrate a high degree of conversion ($>95\%$) from linear to circular polarization at 0.65 THz. The Stokes parameters shown in figure 6 indicate a reflectivity of $>95\%$ and almost $\sim 100\%$ circular polarized THz radiation under the “no light,” or “on,” condition. When the resonance is turned “off,” or under the “light” condition, the reflectivity is $>75\%$ and the THz radiation is almost 100% linearly polarized.

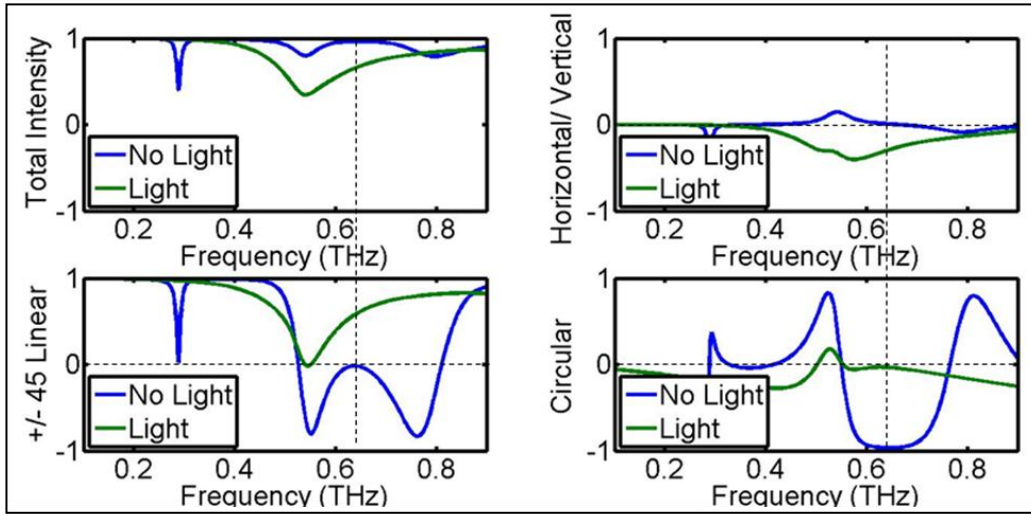


Figure 6. Stokes parameters of the optically modulated QWP shown in figure 5a.

Simulations of the electrically modulated QWPs show good conversion from linear to circular polarization at 0.55 THz. Figure 7 displays the Stokes parameters for the doped, or resonance “off,” and undoped, or resonance “on,” conditions. When the gap region is undoped, >90% of the THz radiation is reflected with mostly (~90%) circular polarization. Under doped conditions, the THz radiation is >50% reflected and mostly (~80%) linearly polarized.

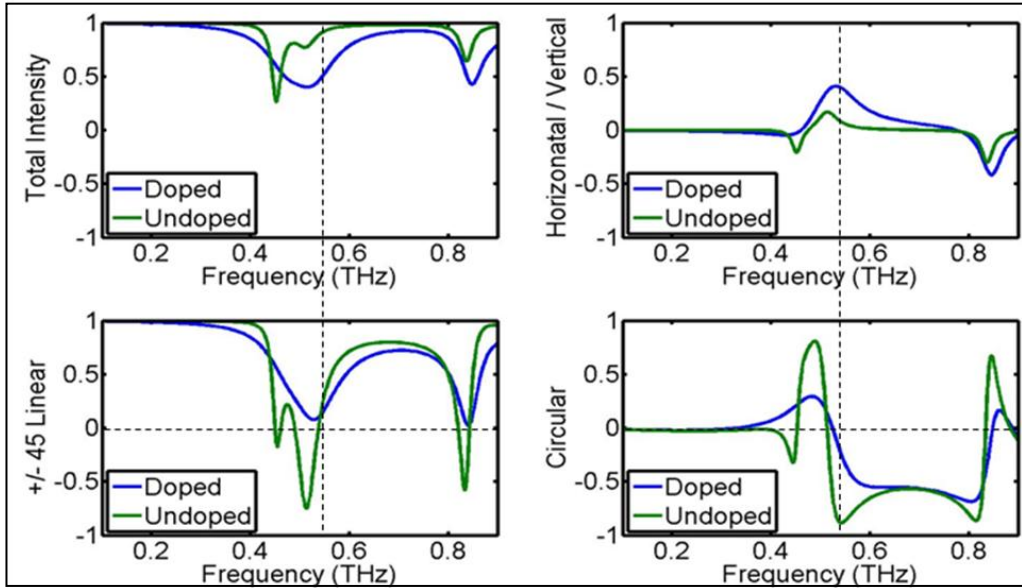


Figure 7. Stokes parameters of the electrically modulated QWP shown in figure 5b.

To improve the polarization conversion of the electrically controlled waveplates, three-dimensional (3-D) structures were investigated, which allow for pure magnetic excitation and a larger design phase space. Figure 8 illustrates (a) the unit cell of the 3-D electrically modulated

QWP and (b) the associated simulated throughput and phase shift. Although we have achieved significant phase shifts (greater than 180°) in static waveplates, the phase shifts with the dynamic waveplates are smaller than expected.

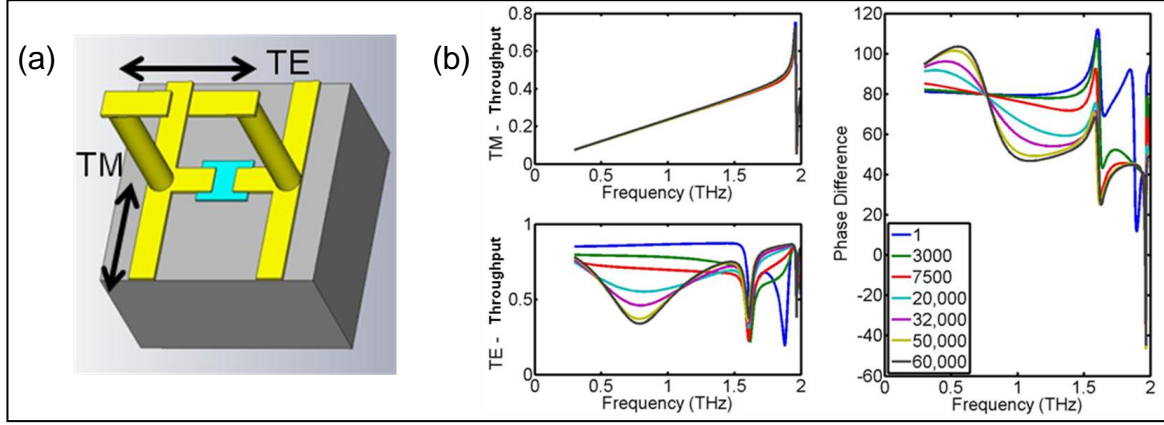


Figure 8. (a) Illustration of the 3-D electrically modulated QWP and (b) simulated transverse magnetic (TM) and transverse electric (TE) mode throughput and phase shift.

Fortunately, our research opened up an additional path whereby dynamic perfect absorbers (PAs) can allow for high contrast control of the polarization. Although this technique absorbs half of the incident intensity, the fabrication strategies are quite similar and PAs can be much simpler to realize than a pure phase control approach. In the second year of the program, the optically modulated PAs shown in figure 9a were fabricated using SRRs on silicon (Si) on sapphire. The material was etched such that Si remained only in the SRR gap. Simulations demonstrate photoexcited electron-hole pairs in Si shorting the gap and turning off the PA resonance at 0.915 THz (figure 9b). As the excitation power (and conductivity) increases, dipole resonances begin to appear at 1.85 and 1.36 THz. Figure 9c shows the experimental characterization using time-resolved THz spectroscopy of our first generation optically modulated PAs. PA resonance effects were observed but were unfortunately convoluted with birefringence effects from the sapphire substrate. Improvements were made in subsequent generation devices discussed below.

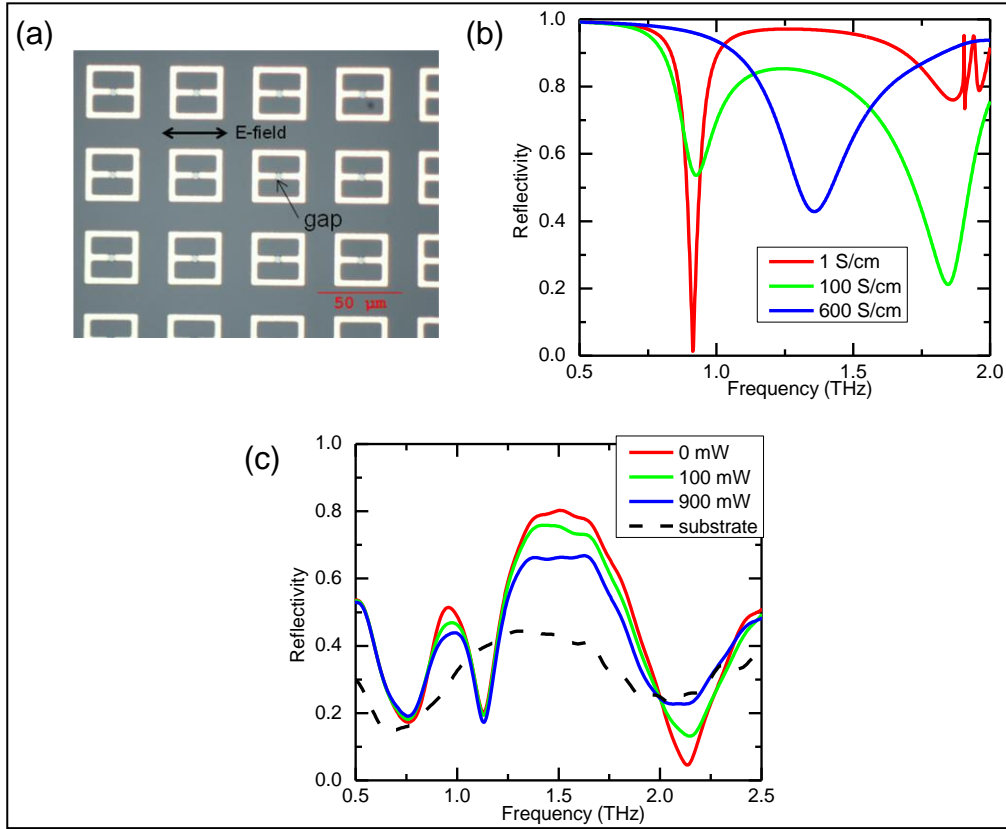


Figure 9. (a) Image of the fabricated optically controlled PA. (b) Simulated and (c) measured reflectivity from the first generation optically controlled PA. A 532-nm CW laser was used for optical biasing.

Figure 10a displays the electrically controlled PAs fabricated using SRR on *n*-type gallium arsenide (GaAs) on semi-insulating GaAs. The *n*-type GaAs is grown by molecular beam epitaxy to a thickness of 2 μm and doping density of $2 \times 10^{16} \text{ cm}^{-3}$. The thin film is etched such that *n*-type GaAs remains only in the gap. As shown in figure 10b, the metamaterial provides the ohmic contact while the gold ground plane functions as the Schottky contact. A reverse bias depletes carriers in the *n*-GaAs gap and turns “on” the PA resonance, as demonstrated in the simulated absorption in figure 10c. Several fabrication challenges were resolved for this device, including improved etching by deposition of a 300-nm aluminum gallium arsenide ($\text{Al}_{0.95}\text{Ga}_{0.05}\text{As}$) etch stop between the doped and undoped GaAs material, as well as fabrication of high aspect ratio post between the *n*-GaAs island and ground plane.

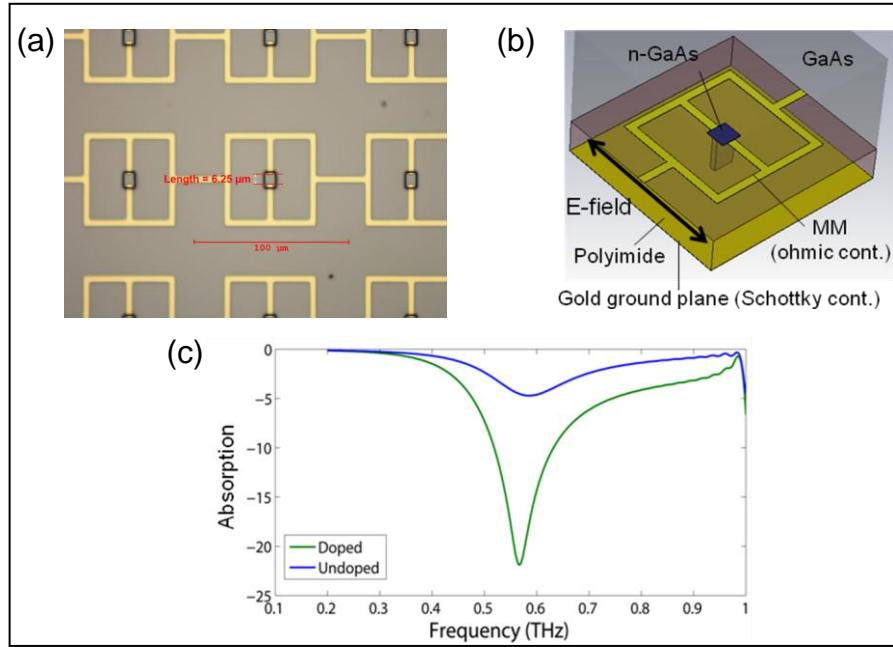


Figure 10. (a) Image of the fabricated electrically controlled PA and (b) schematic of the unit cell, and plot of the simulated absorption.

In the last year of our program, second-generation devices were designed to offset the sapphire crystal axes with those of the SRR to minimize birefringence effects in the optically controlled PAs. Fabrication techniques were also improved to etch a cleaner Si island at the SRR gap. Figure 11 shows the improved reflectivity measured using CW THz spectroscopy of the second generation optically modulated PAs. Third-generation optically controlled PAs (figure 12a) further improved the device performance by matching the free space impedance. Figure 12 shows excellent correlation between the (b) experimental and (c) simulated results. The third-generation devices demonstrated a broadened resonance frequency band (0.8 to 1.2 THz) ideal for operation with the bandwidth of high resolution Schottky diodes.

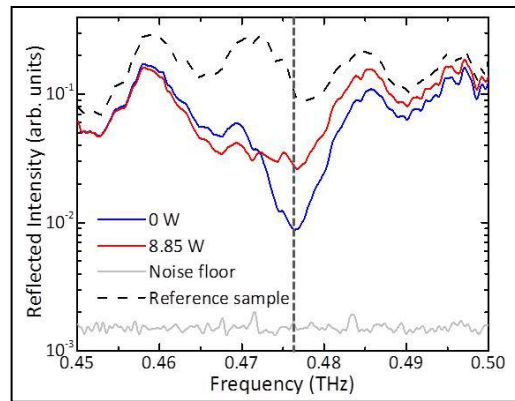


Figure 11. Plot of the experimentally measured reflectivity from the second-generation optically controlled perfect absorber.

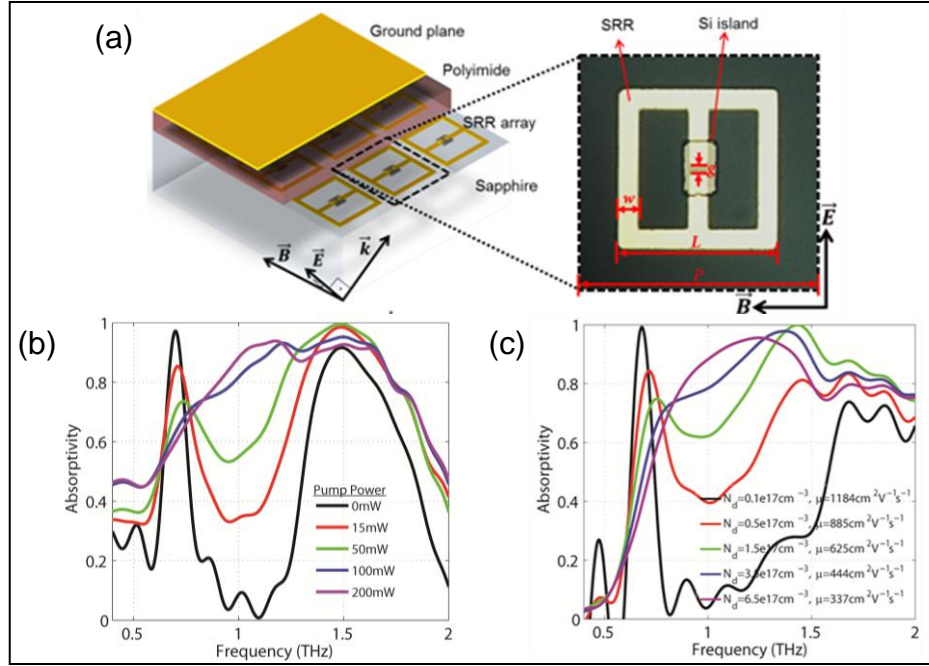


Figure 12. (a) Illustration and scanning electron microscopy (SEM) image of third-generation optically controlled PA. (b) Experimental and (c) simulated performance of the PA.

The wide tunability of our polarimeter demands metamaterial devices with frequency tunability as well. To this end, we have demonstrated ~30% resonant frequency shift and bandwidth broadening through capacitance tuning of dual gap SRRs. Figure 13 illustrates the fabricated optically controlled 3-D structures along with the measured and simulated spectra. The operational frequency of the metamaterials can be easily designed to match the Schottky diode bands.

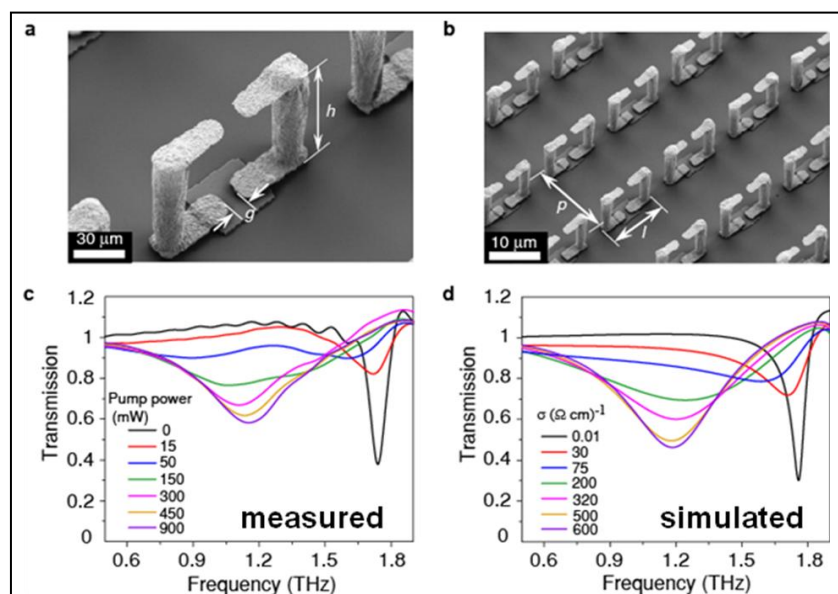


Figure 13. Image of the optically controlled (a) unit cell and (b) array of the dual gap frequency tunable metamaterial. Plot of the (a) measured and simulated transmission spectra.

The metamaterial devices developed here will not only provide active THz polarization control to enable THz polarimetry for spectroscopic detection of chemical and biological threat analytes, but can easily be extended onto other platforms for applications such as high bandwidth communications at THz frequencies.

4. Opportunities for Training and Professional Development Provided by the Project

Our research project provided an ideal training and professional development environment for graduate students as well as postdoctoral fellows. At Boston University, the project funded four graduate students in their Ph.D. studies, two of which obtained their Ph.D.s during the course of the project. The graduate students participated in all facets of the research: from metamaterial device design and fabrication to testing using THz spectroscopy. These students published scientific papers in peer-reviewed journals, obtained advanced technical training in multidisciplinary research, and further disseminated their results at international conferences. At ARL, the project funded a postdoctoral fellow who played a role in designing and building the metamaterial-based THz polarimeter as well as the characterizing and analyzing the metamaterials.

5. Dissemination to Communities of Interest

Besides the publications and presentations detailed in section 7, our results have been disseminated through lab tours to high school students (Junior Science and Humanities Symposium) and visiting researchers, as well as private communications between colleagues.

6. Personnel Supported

This project supported the following personnel:

- ARL: 2 staff research scientists (Drs. Grace Metcalfe and Michael Wraback) and 1 postdoctoral fellow (Dr. Nathaniel Woodward)
 - Boston University: 2 faculty professors (Drs. Richard Averitt and Xin Zhang) and 4 graduate students (Andrew Strikwerda and Kebin Fan, 2010–2012, and Huseyin Seren and George Keiser, 2012–2013)
-

7. Impact

7.1 Publications

The following publications resulted from this project:

- Fan, K.; Zhao, X.; Zhang, J.; Geng, K.; Keiser, G.; Seren, H.; Metcalfe, G. D.; Wraback, M.; Zhang, X.; Averitt, R. D. Optically Tunable Terahertz Metamaterials on Highly Flexible Substrates. invited submission to *IEEE Transactions on Terahertz Science and Technology*, 2013.
- Keiser, G.; Strikwerda, A.; Fan, K.; Young, V.; Zhang, X.; Averitt, R. Decoupling Crossover in Asymmetric Broadside Coupled Split Ring Resonators at Terahertz Frequencies. *Phys. Rev. B* **2013**, 88, 024101.
- Fan, K.; Strikwerda, A. C.; Zhang, X.; Averitt, R. D. Three-Dimensional Broadband Tunable Terahertz Metamaterials. *Physical Review B – Rapid Communications* **2013**, 87, 161104.

- Seren, H. R.; Strikwerda, A. C.; Cao, L.; Keiser, G. R.; Zhang, J.; Fan, K.; Metcalfe, G. D.; Wraback, M.; Averitt, R. D.; Zhang, X. An Optically Tunable Terahertz Perfect Absorber. *Proceeding of the 17th International Conference on Solid-State Sensors, Actuators and Microsystems (Transducers '13)*, 2013, pp. 1428–1431.
- Fan, K.; Zhao, X.; Zhang, J.; Metcalfe, G. D.; Averitt, R. D.; Zhang, X. Flexible and Tunable Metamaterials at Terahertz Frequencies. *Proceedings of the 17th International Conference on Solid-State Sensors, Actuators and Microsystems (Transducers '13)*, 2013, pp. 2225–2228.
- Brandt, N. C.; Hwang, H. Y.; Fan, K.; Averitt, R. D.; Zhang, X.; Nelson, K. A. Nonlinear 2D and 3D Metamaterials on Silicon. *Proceedings of the International Workshop on Optical Terahertz Science and Technology*, 2013.
- Hwang, H. Y.; Liu, M.; Fan, K.; Zhang, J.; Strikwerda, A. C.; Sternbach, A.; Brandt, N. C.; Perkins, B. G.; Zhang, X.; Averitt, R. D.; Nelson, K. A. Metamaterial-Enhanced Nonlinear Terahertz Spectroscopy. *EPJ Web Conferences, XVIIIth International Conference on Ultrafast Phenomena*, 41, 09005, 2013.
- Iwaszczuk, K.; Strikwerda, A.; Fan, K.; Zhang, X.; Averitt, R.; Jepsen, P. Flexible Metamaterial Absorbers for Stealth Applications at Terahertz Frequencies. *Optics Express* **2012**, 20 (1), 635–643.
- Metcalfe, G. D.; Wraback, M.; Strikwerda, A. C.; Fan, K.; Zhang, X.; Averitt, R. D. Terahertz Polarimetry Based on Metamaterial Devices. *Proc. SPIE* Vol. 8363, 83630O, 2012.
- Fan, K.; Strikwerda, A. C.; Averitt, R. D.; Zhang, X. Three-Dimensional Magnetic Terahertz Metamaterials Using a Multilayer Electroplating Technique. *J. Micromechanics and Microengineering* **2012**, 22, 045011.
- Fan, K.; Strikwerda, A. C.; Tao, H.; Zhang, X.; Averitt, R. D. Stand-Up Magnetic Metamaterials at Terahertz Frequencies. *Optics Express* **2011**, 19, 12619.
- Ekmekci, E.; Strikwerda, A. C.; Fan, K.; Keiser, G. R.; Zhang, X.; Turhan-Sayan, G.; Averitt, R. D. Frequency Tunable Terahertz Metamaterials Using Broadside Coupled Split-Ring Resonators. *Phys. Rev. B* **2011**, 83, 193103.
- Strikwerda, A. C.; Fan, K.; Metcalfe, G. D.; Wraback, M.; Zhang, X.; Averitt, R. D. Electromagnetic Composite-Based Reflecting THz Waveplates. *International J. High Speed Electronics and Systems* **2011**, 20 (3), 583–588.

- Strikwerda, A. C.; Fan, K.; Metcalfe, G. D.; Wraback, M.; Zhang, X.; Averitt, R. D. Electromagnetic Composite-Based Reflecting Terahertz Waveplates. *Proceedings of the International Workshop on Optical Terahertz Science and Technology*, 2011.

7.2 Participation/Presentations at Meetings, Conferences, Seminars, etc.

The following participation/presentations resulted from this project:

- Seren, H. R.; Strikwerda, A. C.; Cao, L.; Keiser, G. R.; Zhang, J.; Fan, K.; Metcalfe, G. D.; Wraback, M.; Averitt, R. D.; Zhang, X. An Optically Tunable Terahertz Perfect Absorber. *17th International Conference on Solid-State Sensors, Actuators and Microsystems (Transducers '13)*, Barcelona, Spain, June 16–20, 2013.
- Fan, K.; Zhao, X.; Zhang, J.; Metcalfe, G. D.; Averitt, R. D.; Zhang, X. Flexible and Tunable Metamaterials at Terahertz Frequencies. *17th International Conference on Solid-State Sensors, Actuators and Microsystems (Transducers '13)*, Barcelona, Spain, June 16–20, 2013.
- Brandt, N. C.; Hwang, H. Y.; Fan, K.; Averitt, R. D.; Zhang, X.; Nelson, K. A. Nonlinear 2D and 3D Metamaterials on Silicon. *International Workshop on Optical Terahertz Science and Technology*, Kyoto, Japan, April 1–5, 2013.
- Keiser, G.; Seren, H.; Zhang, X.; Averitt, R. Controlling Metamaterial Field Enhancement at THz Frequencies. *March Meeting of the American Physical Society*, Baltimore, MD, March 2013.
- Hwang, H. Y.; Liu, M.; Fan, K.; Zhang, J.; Strikwerda, A. C.; Sternbach, A.; Brandt, N. C.; Perkins, B. G.; Zhang, X.; Averitt, R. D.; Nelson, K. A. Metamaterial-Enhanced Nonlinear Terahertz Spectroscopy. *EPJ Web Conferences, XVIIIth International Conference on Ultrafast Phenomena*, Lausanne, Switzerland, July 2012.
- Metcalfe, G. D.; Wraback, M.; Strikwerda, A. C.; Fan, K.; Zhang, X.; Averitt, R. D. Terahertz Polarimetry Based on Metamaterial Devices. *SPIE Defense, Security and Sensing Conference*, Baltimore, MD, April 2012.
- Strikwerda, A. C.; Fan, K.; Metcalfe, G. D.; Woodward, N.; Wraback, M.; Zhang, X.; Averitt, R. D. Metamaterial-Based Terahertz Polarimetry for Enhanced Chem.-Bio Detection. *Chemical and Biological Defense Science and Technology Conference*, Las Vegas, NV, November 2011.
- Fan, K.; Strikwerda, A.; Zhang, X.; Averitt, R. D. A Tunable 3D Metamaterial, invited talk at *Infrared and Millimeter Waves 2011*, Houston, TX, October 2011.

- Averitt, R. D. Prospect of Terahertz Metamaterials, invited talk at *Terahertz Castle Meeting*, Marburg, Germany, July 6th, 2011.
- Fan, K.; Strikwerda, A.; Zhang, X.; Averitt, R. D. A Tunable 3D Metamaterial, poster presented at *Surface Plasmon Polaritons 5*, Busan Korea, May 2011.
- Strikwerda, A. C.; Ekmekci, Evren; Fan, K.; Keiser, G.; Zhang, Xin; Turgan-Sayan, G.; Averitt, Richard D. Frequency Tunable Metamaterial Designs Using Near Field Coupled SRR Structures in the Terahertz Region. *Conference on Lasers and Electro-Optics*, Baltimore, MD, May 2011.
- Strikwerda, A. C.; Fan, K.; Metcalfe, G. D.; Wrbach, M.; Zhang, X.; Averitt, R. D. Electromagnetic Composite-Based Reflecting Terahertz Waveplates. *Optical Terahertz Science and Technology*, Santa Barbara, CA, March 2011.
- Strikwerda, A. C.; Fan, K.; Metcalfe, G. D.; Wrbach, M.; Zhang, X.; Averitt, R. D. Reflecting THz Waveplates. *IEEE Lester Eastman Conference on High Performance Devices*, Troy, NY, August 2010.

7.3 New Discoveries, Inventions, or Patent Disclosures

The following also resulted from this project:

- Non-provisional U.S. patent filed August 3, 2012, application #13566452, G.D. Metcalfe, M. Wrbach, A. C. Strikwerda, R. D. Averitt, K. Fan, and X. Zhang, “Electromagnetic Composite-based reflecting terahertz waveplate.”

7.4 Honors/Awards

The following honor/award resulted from this project:

- Ph.D. received by Boston University students Andrew Strikwerda and Kebin Fan, May 2012.

7.5 Courses Taught

The following course resulted from this project:

- Physics 897: “Introduction to Metamaterials” taught by Prof. Averitt at Boston University, Fall 2011.

8. Conclusion

The functionally active metamaterial devices developed here will not only provide active THz polarization control to enable THz polarimetry for spectroscopic detection of chemical and biological threat analytes, but can easily be extended onto other platforms for applications such as high bandwidth communications at THz frequencies.

List of Symbols, Abbreviations, and Acronyms

3-D	three-dimensional
ARL	U.S. Army Research Laboratory
CW	continuous-wave
GaAs	gallium arsenide
HWPs	half waveplates
PA	perfect absorber
QWPs	quarter waveplates
SEM	scanning electron microscopy
Si	silicon
SNR	signal-to-noise ratio
SRR	split-ring resonator
TE	transverse electric
THz	terahertz
TM	transverse magnetic

1 DEFENSE TECH INFO CTR
(PDF) ATTN DTIC OCA (PDF)

2 US ARMY RSRCH LABORATORY
(PDF) ATTN IMAL HRA MAIL & RECORDS MGMT
ATTN RDRL CIO LL TECHL LIB

1 GOVT PRNTG OFC
(PDF) ATTN A MALHOTRA

1 U.S. ARMY RSRCH LAB
(PDF) ATTN RDRL SEE M
G D METCALFE

INTENTIONALLY LEFT BLANK.